Comparison of the Structure and Evolution of Intraseasonal Oscillations Before and After Onset of the Asian Summer Monsoon

QI Yanjun* (齐艳军), ZHANG Renhe (张人禾), ZHAO Ping (赵 平), and ZHAI Panmao (翟盘茂)

Chinese Academy of Meteorological Sciences, Beijing 100081

(Received December 25, 2012; in final form July 1, 2013)

ABSTRACT

High-resolution satellite-derived data and NCEP-NCAR reanalysis data are used to investigate intraseasonal oscillations (ISO) over the tropical Indian Ocean. A composite evolution of the ISO life cycle is constructed, including the initiation, development, and propagation of rainfall anomalies over the tropical Indian Ocean. The characteristics of ISO over the tropical Indian Ocean are profoundly different before and after the onset of the Indian summer monsoon. Positive precipitation anomalies before monsoon onset appear one phase earlier than those after monsoon onset. Before monsoon onset, precipitation anomalies associated with ISO first initiate in the western tropical Indian Ocean and then propagate eastward along the equator. After monsoon onset, convective anomalies propagate northward over the Indian summer monsoon region after an initial eastward propagation over the equatorial Indian Ocean. Surface wind convergence and air-sea interaction play critical roles in initiating each new cycle of ISO convection.

Key words: tropical Indian Ocean, intraseasonal oscillation, Asian summer monsoon, onset

Citation: Qi Yanjun, Zhang Renhe, Zhao Ping, et al., 2013: Comparison of the structure and evolution of intraseasonal oscillations before and after onset of the Asian summer monsoon. *Acta Meteor. Sinica*, **27**(5), 684–700, doi: 10.1007/s13351-013-0511-2.

1. Introduction

Intraseasonal oscillation (ISO) is one of the most significant modes of variability in the tropical atmosphere. This oscillation was first detected by Madden and Julian in the early 1970s (Madden and Julian, 1971, 1972) and is now often referred to as the Madden-Julian Oscillation (MJO). The major features of the observed MJO include eastward propagation with a zonal wavenumber-1 structure and a period of 45–50 days. This characteristic oscillation is most frequently observed during boreal winter, with eastward propagation considerably weakened during boreal summer (Wang and Rui, 1990; Jiang et al., 2004; Lin and Li, 2008). The atmospheric ISO propagates northward in the Indian monsoon sector and northwestward off the equator in the western Pacific during boreal summer (Yasunari, 1979, 1980; Lau and Chan, 1986; Wang and Rui, 1990; Wang and Xu, 1997). The MJO signal appears in a wide variety of meteorological variables, including wind, surface air pressure, cloud amount, outgoing longwave radiation (OLR), precipitation, and water vapor (Madden and Julian, 1971, 1972; Murakami, 1976; Yasunari, 1979; Wang and Rui, 1990; Guan et al., 1995; Zhan et al., 2006). The northward propagation of the boreal summer ISO over the South Asian monsoon region was first described by Yasunari (1979). This northward propagation from the equatorial ocean toward the South Asian subcontinent is often associated with transitions between active and break cycles of the Indian monsoon (Yasunari, 1979, 1980; Sikka and Gadgil, 1980; Krishnamurti and Subrahmanyam, 1982; see also review by Li and Wang, 2005). A large number of studies have documented close relationships between ISO propagation in the eastern Indian Ocean and western Pacific and local

Supported by the National Basic Research and Development (973) Program of China (2012CB417205), National Natural Science Foundation of China (41221064), and Basic Research Fund of the Chinese Academy of Meteorological Sciences (2009Y006 and 2010Z003).

*Corresponding author: qiyj@cams.cma.gov.cn.

©The Chinese Meteorological Society and Springer-Verlag Berlin Heidelberg 2013

weather and climate anomalies in South and Southeast Asia (Shukla and Paolino, 1983; Huang, 1994; Goswami and Mohan, 2001; Zhu et al., 2003; Ju and Zhao, 2005; Li et al., 2005; Wang et al., 2005).

The northward propagation of ISO over the South Asian monsoon region is intimately related to fluctuations in Indian summer monsoon precipitation anomalies (i.e., active and break phases of the monsoon) with a characteristic period of 30–40 days (Krishnamurti and Bhalme, 1976; Gadgil, 2003). Strong interannual variations in the propagation and intensity of boreal summer ISO may cause changes in the duration of the rainy or dry season in the Indian summer monsoon region (Mehta and Krishnamurti, 1988; Hendon et al., 1999; Kemball-Cook and Wang, 2001; Kripalani et al., 2004). Interannual variations in sea surface temperature (SST) in the Indian Ocean can also affect the meridional propagation and intensity of ISO (Rao and Yamagata, 2004; Yang et al., 2007; Lin et al., 2010, 2011). Variability in ISO activity in the tropical Indian Ocean has a substantial impact on monsoon cycles in South Asia.

Previous studies have shown that the eastern equatorial Indian Ocean (EEIO) is a center of strong ISO variability and a preferred region for ISO amplification (Murakami et al., 1986; Wang and Rui, 1990). Interannual variations of ISO intensity over the tropical Indian Ocean appear to be controlled in part by changes in mean convective activity over the EEIO (Li et al., 2003; Teng and Wang, 2003; Qi et al., 2008). Changes in the intensity and propagation of ISO over the tropical Indian Ocean may in turn affect the onset and retreat of the Indian summer monsoon (Yasunari, 1979, 1980; Krishnamurti and Subrahmanyam, 1982; Li et al., 2013), as nonlinear eddy momentum transport associated with ISO contributes significantly to the development of low-level westerlies during the onset and initial development of the monsoon (Qi et al., 2009). ISO convective anomalies during boreal summer first initiate in the western and central equatorial Indian Ocean (Jiang and Li, 2005; Wang et al., 2005), and then propagate eastward along the equator (Jiang et al., 2004; Wang et al., 2006). These anomalies then tend to turn northward as they approach the Maritime Continent. However, several open questions remain. For instance, does ISO activity differ significantly between the periods before and after the onset of the Indian summer monsoon? Do the structure and evolution of ISO before monsoon onset resemble the structure and evolution of ISO after monsoon onset? Motivated by these questions, we use a suite of satellite and other observational datasets to investigate the temporal and spatial structures of ISO over the tropical Indian Ocean.

2. Data and methods

High-resolution satellite data have been widely applied in studies of ISO and monsoons in recent years. These data compensate for the lack of traditional meteorological data over the tropical oceans (Wang et al., 2005, 2006). The Tropical Rainfall Measuring Mission (TRMM) Microwave Imager (TMI) provides observations of a variety of parameters, including precipitation rate, SST, and cloud liquid water. Here, we use daily estimates of precipitation rate and SST derived from TMI at a horizontal resolution of $0.25^\circ \times 0.25^\circ$. We also use daily sea surface winds derived from NASA JPL QuikSCAT scatterometer observations at a resolution of $0.5^\circ \times 0.5^\circ$. We describe the vertical structure of the ISO using daily mean estimates of specific humidity and vertical velocity from the NCEP-NCAR reanalysis, at a resolution of $2.5^\circ \times 2.5^\circ$.

We isolate the ISO signal by applying a bandpass filter to each meteorological variable at each pressure level. A total of 7–12 harmonics are extracted for each year, corresponding to periods of 20–50 days. We construct a composite analysis of each phase to describe the structure and evolution of ISO cycles over the tropical Indian Ocean. The analysis period extends from 1998 to 2005. The statistical significance of the composite ISO cycles is evaluated using a Student's t-test.

3. Variance of summertime ISO over EEIO

The EEIO west of Sumatra is a permanent center of convective activity during boreal summer on both seasonal and intraseasonal timescales (Yasunari, 1979; Sikka and Gadgil, 1980; Kemball-Cook and Wang,

2001; Teng and Wang, 2003; Wang et al., 2005). The dominant periods of ISO in this region vary from boreal winter to summer. For example, the dominant period of the MJO during boreal winter is approximately 50 days, but this period is shortened to approximately 35 days during boreal summer (Hartmann et al., 1992; Wang et al., 2005, 2006). The dominant period over the EEIO is 20–50 days during boreal summer. Wang et al. (2005, 2006) showed that fluctuations that occur at periods of 20–50 days account for 60%–70% of the total variance of daily precipitation over the EEIO. We have verified that the fraction of variance accounted for by the 20–50-day band is predominant over the EEIO during boreal summer in the data we use. This result indicates that the EEIO is a preferred region for ISO variability with a period of 20–50 days. For the remainder of this study, we will focus exclusively on ISO with periods of 20–50 days.

We identify the center of ISO activity during boreal summer by calculating the variances of both daily precipitation (with the seasonal cycle removed) and 20–50-day bandpass-filtered TMI precipitation. Both variances are calculated for the period from May to September. The distribution of variance (Fig. 1) indicates that maxima in ISO activity occur over the EEIO and the South China Sea. TMI precipitation averaged over the eastern equatorial Indian Ocean (5°S–5°N, 75°–100°E) is selected as the reference time series to account for the link between variations of convection over the EEIO and anomalies in rainfall over the Indian monsoon region (Teng and Wang, 2003; Qi et al., 2008). We then describe the structural evolution of ISO in this region using the 20–50-day filtered time series. This approach enables us to evaluate the characteristics of ISO initiation, amplification, and propagation both before and after the onset of the Indian summer monsoon.

The time series of daily mean and 20–50-day filtered precipitation anomalies over the EEIO (Fig. 2) include several transitions between active and break phases. We construct the composite analysis using only those ISO cases with amplitudes exceeding one (or negative one) standard deviation. Each selected ISO cycle was divided into eight consecutive phases. The composites were constructed separately for periods before and after monsoon onset in order to best describe the distinctive behavior of ISO over the tropical Indian Ocean during each period.

The statistical long-term mean date of summer monsoon onset over southwestern India (Kerala) is 1 June, with a standard deviation of 8 days (Joseph et al., 1994). The two vertical lines shown in Fig. 2 represent the earliest and latest dates of Indian summer monsoon onset, respectively. The ISO cycles chosen for creating composites of ISO evolution before and after monsoon onset are selected according to the estimated onset dates for each year from 1998 to 2005. These selected ISO cycles in the EEIO are in response to significant northward-propagating convective rainfall anomalies associated with the active/break spells of the Indian summer monsoon rainfall (figure omitted).

We regard an ISO cycle as the period from a negative peak through a positive peak and then back to a negative peak (Fig. 2). The first negative peak of each ISO cycle is defined as Phase 1, the first instance of zero amplitude is defined as Phase 3 and the positive peak is defined as Phase 5. The composite ISO cycle is thus broken down into a total of eight phases (the phase after Phase 8 is identical to Phase 1). This phase composite strategy is the same as that used by Wang et al. (2005, 2006). A total of 27 cycles with sufficiently large amplitude are identified in the time

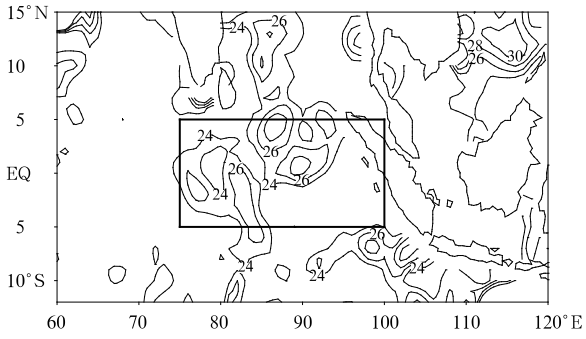

Fig. 1. Spatial distribution of the fraction of variance (%) in deseasonalized daily mean precipitation explained by fluctuations on 20–50-day timescales during boreal summer (May–September) 1998–2005.

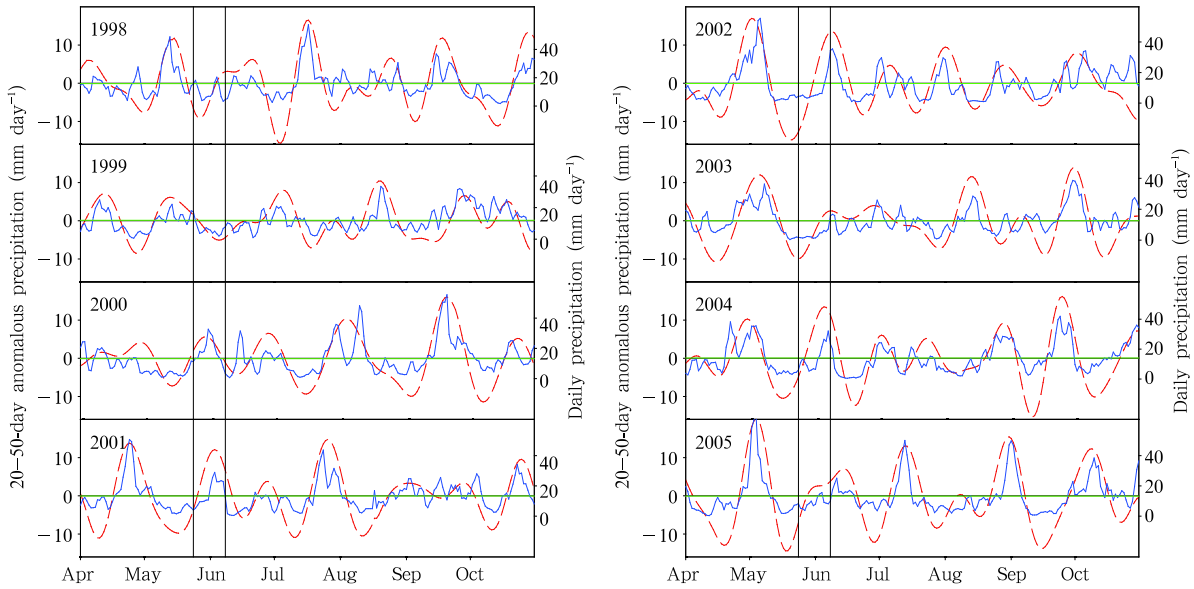

Fig. 2. Time series of area-averaged 20–50-day filtered anomalous precipitation rate (mm day^{-1}; dashed lines) and deseasonalized daily precipitation rate anomalies (mm day^{-1}; solid lines) during boreal summer from 1998 to 2005.

series, including 7 cycles that occurred before monsoon onset and 20 cycles that occurred after monsoon onset. Two eight-phase composites are constructed, one for the 7 cycles identified before monsoon onset and one for the 20 cycles identified after monsoon onset. This approach enables a discussion of similarities and differences in ISO evolution before and after the onset of the monsoon.

4. Structure and evolution of ISO before and after monsoon onset

The purpose of this analysis is to characterize the initiation, development, and propagation of ISO over the tropical Indian Ocean. The high-resolution satellite estimates of daily precipitation rate and SST introduced in Section 2 are used to depict the spatiotemporal evolution of an ISO life cycle. We describe the evolution of the precipitation anomalies in detail for each of the eight phases and document differences between the periods before and after monsoon onset.

4.1 Characteristics of ISO precipitation anomalies before monsoon onset

4.1.1 Initiation of ISO precipitation anomalies

Figure 3 shows the composite life cycle (eight phases) of ISO anomalies in precipitation and SST in the tropical Indian Ocean region be fore monsoon onset. Phases 1 and 2 represent the initial stages of the ISO cycle. Negative precipitation anomalies dominate the central and eastern equatorial Indian Ocean east of 65°E during Phase 1. The largest negative precipitation anomalies occur in the eastern equatorial Indian Ocean near 90°E. The dry anomalies move eastward along the equator during Phase 2, with the maximum negative anomalies located in the eastern Indian Ocean to the west of Sumatra. Meanwhile, a positive precipitation anomaly emerges in the western equatorial Indian Ocean near 55°–70°E.

4.1.2 Enhancement and maturation of ISO precipitation anomalies

The positive precipitation anomalies strengthen considerably during Phase 3. These positive anomalies (with typical precipitation rates exceeding 6 mm day^{-1}) expand eastward along the equator from the western equatorial Indian Ocean near 60°E. Negative precipitation anomalies in the eastern equatorial Indian Ocean grow progressively weaker, then largely disappear in Phase 4 as enhanced positive anomalies expand to cover the entire equatorial Indian Ocean. The maximum positive precipitation anomalies during Phase 4 are located in the eastern Indian Ocean

east of 80°E (Fig. 3). The ISO precipitation anomalies continue to move eastward along the equator into Phase 5, with positive anomalies in the EEIO reaching peak precipitation rates larger than 18 mm day^{-1} near 82°–85°E in Phase 5. The spatial pattern of precipitation during Phase 5 is nearly the mirror image of that during Phase 1 with respect to the sign of the precipitation anomalies. Phase 5 represents the peak precipitation phase in the eastern equatorial Indian Ocean.

4.1.3 Weakening of ISO precipitation anomalies

The positive precipitation anomalies associated with ISO start to move northwestward and southwestward in Phase 6, forming a V shape (Fig. 3). The northern branch of the rainband is much stronger than the southern branch, possibly due to a hemispheric asymmetry in the vertical shear of the background easterly winds and the spatial distribution of SST (Li

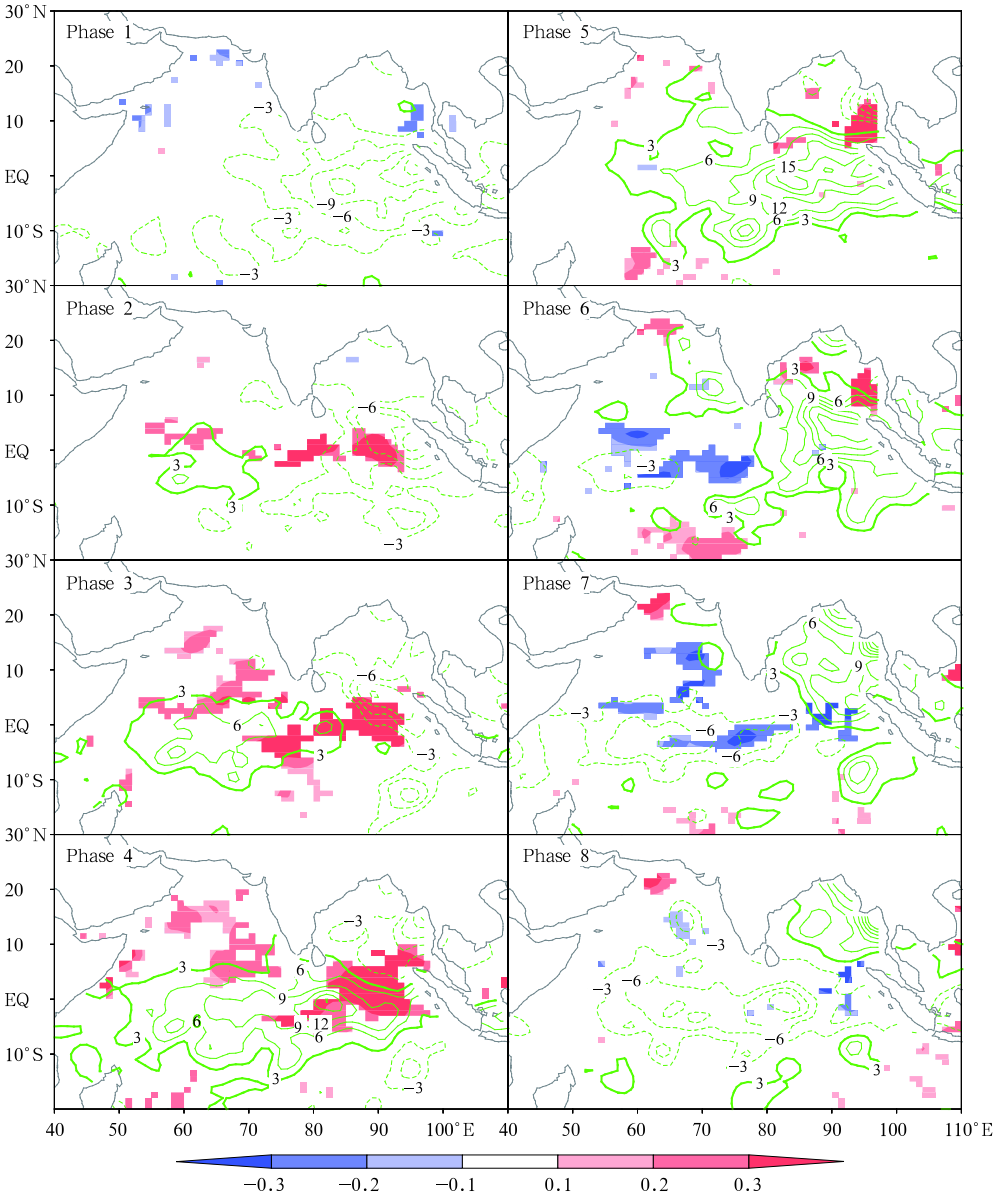

Fig. 3. Composite life cycle of 20–50-day filtered precipitation rate and sea surface temperature (SST) before onset of the Indian summer monsoon. The green contours represent precipitation anomalies starting from ±3 mm day^{-1} with a contour interval of 3 mm day^{-1}. The shading represents SST anomalies in unit of ℃.

and Wang, 1994; Wang and Xie, 1997; Kemball-Cook and Wang, 2001; Lawrence and Webster, 2001; Fu et al., 2003). Stronger easterly vertical shear favors stronger westward-propagating equatorial Rossby waves and deep convection in the Northern Hemisphere (Wang and Xie, 1996). High SST and high specific humidity in the northern Indian Ocean basin are also favorable for Rossby wave generation and deep convection (Li and Wang, 1994; Wang and Xie, 1997). The northern rainband is oriented northwest–southeast during Phases 6–8. Negative precipitation anomalies are generated in the western equatorial Indian Ocean (50°–60°E) starting from Phase 6. The subsequent evolution of these negative precipitation anomalies is similar to that of the positive anomalies during Phases 2–4. The lifecycle of ISO precipitation before monsoon onset is therefore mainly characterized by alternating eastward-propagating precipitation anomalies.

4.2 Characteristics of ISO precipitation anomalies after monsoon onset

4.2.1 Initiation of ISO precipitation anomalies

Figure 4 shows the composite life cycle of ISO precipitation and SST anomalies over the tropical Indian Ocean after monsoon onset. Negative ISO precipitation anomalies dominate the central and eastern equatorial Indian Ocean during Phase 1. The ISO convective precipitation anomaly in the EEIO is out of phase with the precipitation anomaly over the South Asian subcontinent (Wang et al., 2005). More specifically, the tropical Indian Ocean experiences less precipitation when precipitation is high over the Indian subcontinent (i.e., an active phase of the summer monsoon) and more precipitation when precipitation is low over the Indian subcontinent (i.e., a break phase). The negative precipitation anomalies in the eastern equatorial Indian Ocean move northward during Phase 2. The convective rainband in the monsoon region also propagates northward at this stage. The first positive anomalies in the ISO precipitation signal appear in the central equatorial Indian Ocean during Phase 3. This result is substantially different from the constructed composite of ISO activity before monsoon onset, in which positive precipitation anomalies appear one phase (about 5 days) earlier. The negative anomalies move northward rather than eastward with the appearance of the positive precipitation anomalies in the central equatorial Indian Ocean during Phase 3. These northward-moving anomalies are responsible for the transition of the Indian summer monsoon from a wet phase (active monsoon) to a dry phase (break monsoon).

4.2.2 Enhancement and maturation of ISO precipitation anomalies

The ISO precipitation anomalies intensify and shift eastward along the equator during Phases 3 and 4. The ISO-related convective precipitation covers a smaller area than that before monsoon onset. Strong convective precipitation is mainly concentrated in the eastern equatorial Indian Ocean east of 70°E. The positive anomaly in the eastern equatorial Indian Ocean reaches its maximum during the mature stage of the ISO (i.e., Phase 5). Meanwhile, negative precipitation anomalies prevail over most parts of the Indian subcontinent and Bay of Bengal. Meridional expansion of ISO convective anomalies over the EEIO during Phases 4 and 5 is much weaker after monsoon onset than before monsoon onset. This difference in the meridional structure of the rainband may be caused by the relative weakness of Rossby wave generation in June–August when compared with that in May (Kemball-Cook and Wang, 2001; Lawrence and Webster, 2001). The area of positive convective anomalies with anomalous precipitation rates exceeding 3 mm day^{-1} during Phases 4 and 5 was also much smaller after monsoon onset than before monsoon onset. After monsoon onset, ISO convective precipitation is mainly confined to the eastern equatorial Indian Ocean (east of 70°E) between 10°S and 10°N. Before monsoon onset, ISO convective precipitation covers the entire central and eastern tropical Indian Ocean (east of 60°E).

4.2.3 Weakening of ISO precipitation anomalies

ISO precipitation anomalies over the EEIO weaken and become negative from Phase 6 to 8. As to ISO activity before monsoon onset, positive anomalies in ISO convective precipitation expand northwestward and southwestward after reaching the eastern equato-

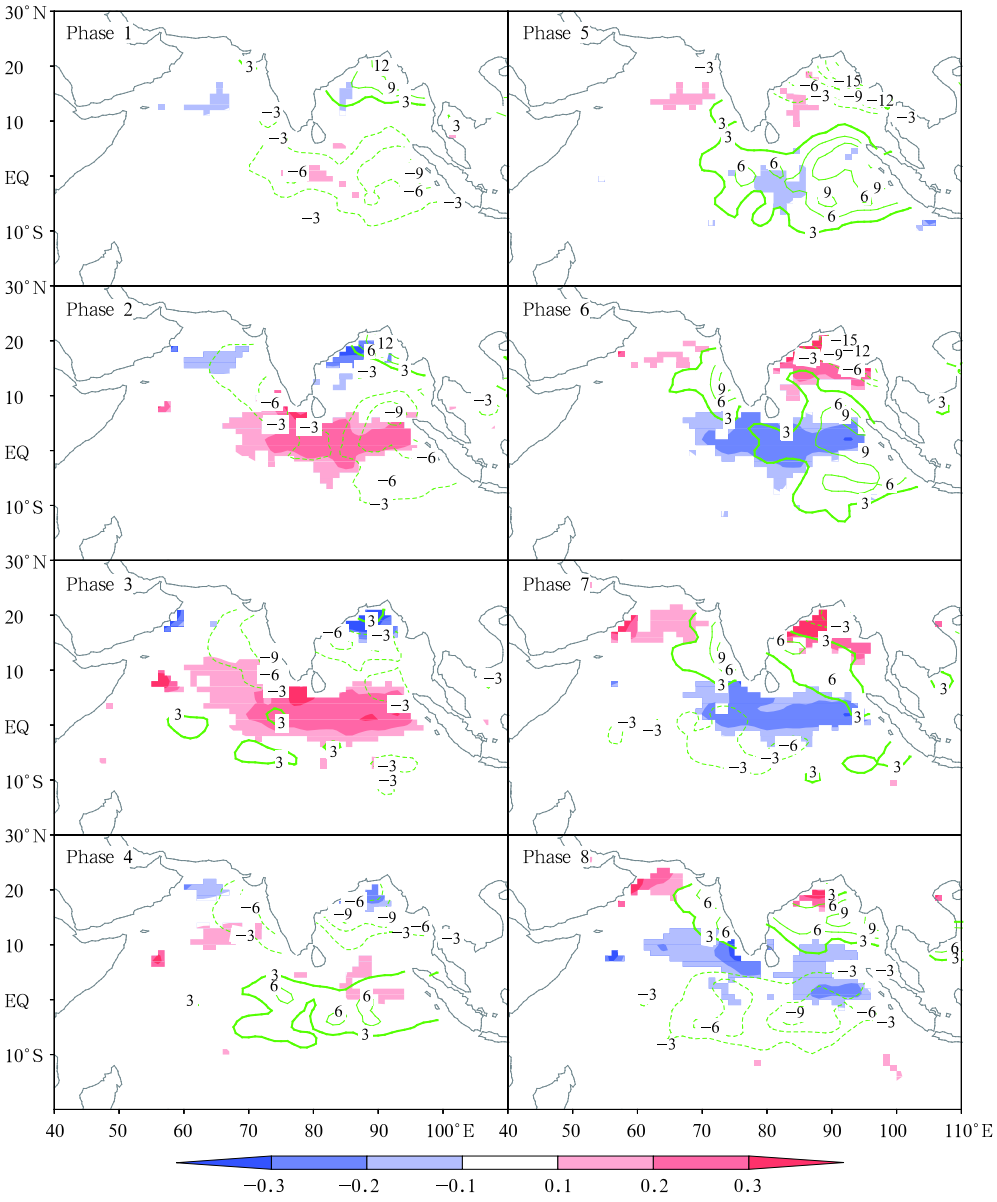

Fig. 4. As in Fig. 3, but for the situation after monsoon onset.

rial Indian Ocean. Unlike ISO activity before monsoon onset, the major center of convective activity continues moving northward away from the equator, while the southern branch weakens rapidly. The northern rainband eventually moves over the Indian subcontinent. The eastern equatorial Indian Ocean is exclusively covered by negative precipitation anomalies as a consequence of this northward propagation, setting the stage for the next phase of the ISO cycle.

The evolution of ISO convective precipitation anomalies before and after monsoon onset can be summarized as follows. Phase 1 is the peak dry phase for the entire central and eastern tropical Indian Ocean. Positive ISO precipitation anomalies appear and begin to develop in the central and western equatorial Indian Ocean during Phases 2 and 3. This development occurs one phase earlier before monsoon onset than after monsoon onset. This difference can be attributed to the monsoon cycle requiring time to spin up during mid and late summer, when upwelling cold water

along the east coast of Africa inhibits the formation of deep convection over the western equatorial Indian Ocean (Webster et al., 1999). ISO convective anomalies in the equatorial Indian Ocean before monsoon onset propagate eastward from initiation, through their development and maturation and to their eventual decay. By contrast, ISO convective anomalies after monsoon onset move primarily northward toward the land, causing alternating dry and rainy periods of the subcontinental monsoon.

4.3 Sea surface temperature anomalies

The evolution of SST anomalies in the eastern equatorial Indian Ocean is largely similar before and after the onset of the monsoon, except that SST anomalies are greater in magnitude before onset than after onset. Positive SST anomalies dominate the central–eastern equatorial Indian Ocean during Phases 1–4 (corresponding to the initiation and development of ISO precipitation anomalies; see Figs. 3 and 4). SST anomalies transit from positive to negative during the peak wet phase over the EEIO (Phase 5), when convective precipitation reaches its maximum value. Negative SST anomalies accompany the weakening of convective precipitation over the EEIO from Phase 6 to 8. Positive SST anomalies are located to the northeast of positive precipitation anomalies from Phases 2 to 5, leading to the northeastward movement of the rainband. During the development stage (i.e., Phases 2 and 3), positive SST anomalies tend to enhance precipitation. Decreases in cloud amount during the dry phase over the central equatorial Indian Ocean (Phase 8 and the following Phase 1 of a new ISO cycle) lead to increases in solar radiation reaching the surface. Reductions in evaporation and entrainment cooling due to decreases in the near-surface wind speed may also play a role by reducing energy loss from the surface. All of these features conspire to warm the sea surface in the EEIO during Phases 2 and 3. Sea surface warming in the Indian Ocean results in large-scale surface moisture convergence. In addition, sensible heat fluxes induced by surface warming tend to warm the air immediately above the surface and reduce the surface pressure. The drop in surface pressure in turn enhances moisture convergence in the boundary layer and promotes organized deep convection. Local air-sea interaction therefore plays an important role in the initiation of each new ISO cycle. These conclusions are consistent with previous studies of summertime ISO in the Northern Hemisphere (Kemball-Cook and Wang, 2001; Fu et al., 2003; Li et al., 2005; Wang et al., 2005).

4.4 Surface wind anomalies

Figures 5 and 6 show composites of ISO anomalies in surface wind and divergence/convergence before and after monsoon onset, respectively. Negative precipitation anomalies correspond to anomalously strong divergence in the surface wind, while positive precipitation anomalies correspond to anomalously strong convergence. In other words, the strength of convection is closely related to convergence/divergence in the surface wind. Significant easterly anomalies during the initiation and developing phases of ISO (Phases 1–3) dominate the surface wind fields over the eastern central equatorial Indian Ocean both before and after the onset of the monsoon (Figs. 5 and 6). These easterlies tend to be even stronger during the initiation and developing phases of ISO (Phases 1–3). These equatorial easterly anomalies correspond to negative anomalies in convective precipitation (Figs. 3 and 4). By contrast, anomalous westerlies prevail over the equatorial Indian Ocean during Phases 5–7. These westerly anomalies correspond to positive precipitation anomalies during Phases 5–7, which are collocated but largely opposite in sign to negative precipitation anomalies during Phases 1–3. Anomalies in the near-surface wind fields are weak during the transition phases (Phases 4 and 8); consequently, no zonal dipole is apparent in the convective precipitation anomalies over the tropical Indian Ocean (Figs. 3 and 4).

The equatorial easterly anomalies north of the equator during Phase 1 are associated with an anomalous anticyclone (Figs. 5 and 6). Wind speeds decrease westward along the equator, favoring boundary layer moisture convergence over the central tropical Indian Ocean. After monsoon onset, anomalous westerlies in the Bay of Bengal north of 10°N are associated with strong precipitation in the monsoon region during Phase 1 (Fig. 6). Moisture convergence

over the western–central equatorial Indian Ocean increases during Phase 2, enhancing convection and resulting in positive precipitation anomalies. Surface moisture convergence and precipitation both continue to increase significantly during Phases 3 and 4 (Figs. 3 and 4). Westerly anomalies along the equator increase from west to east during Phase 5 (Figs. 5 and 6) when positive precipitation anomalies over the EEIO are the largest in magnitude. An anomalous cyclonic circulation appears to the north of the center of convective activity, with easterly anomalies to the north of the convection and westerly anomalies both within and to the south of the convection. These results indicate that surface wind and moisture convergence play a critical role in initiating and organizing the ISO convection.

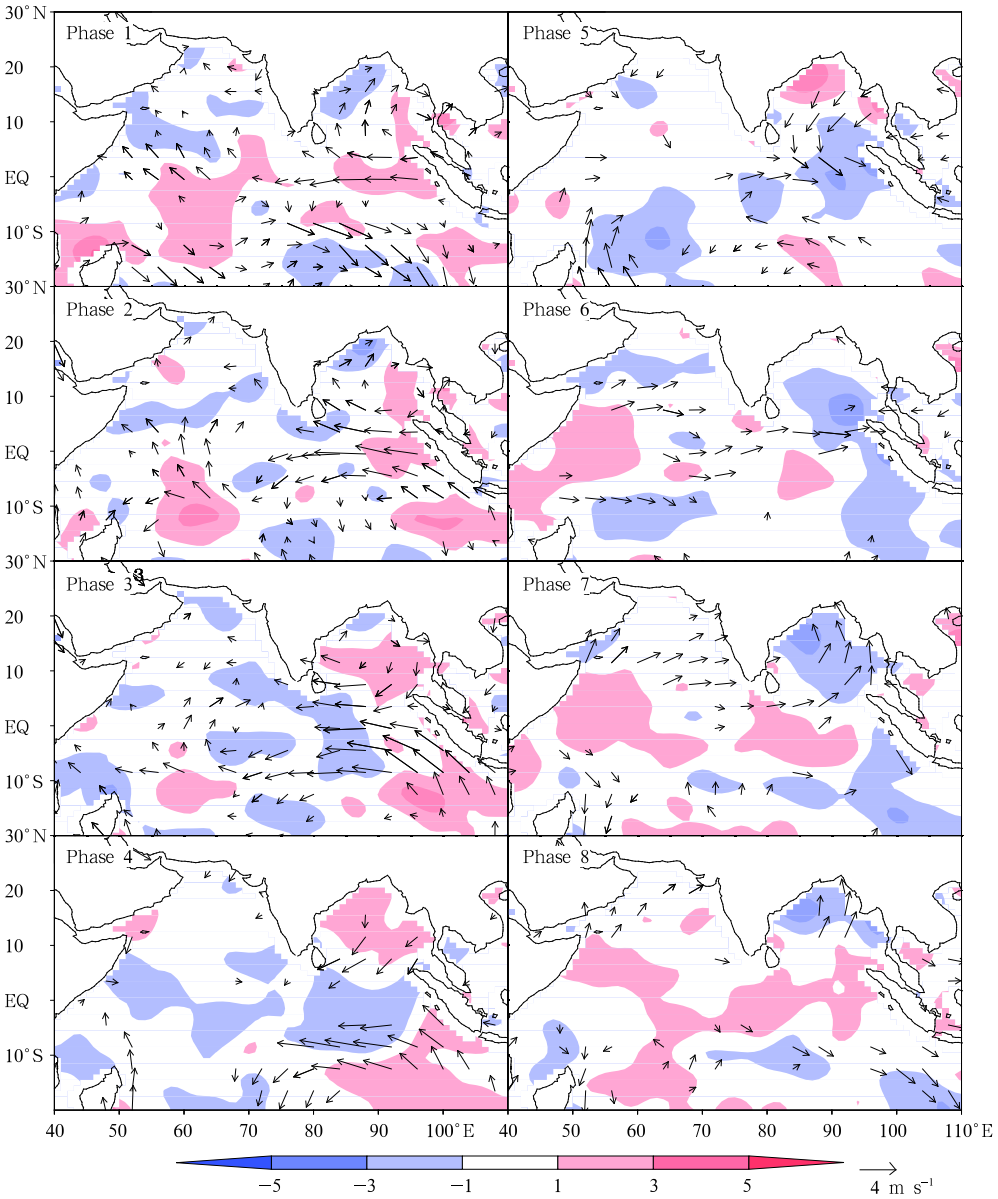

Fig. 5. Composite of anomalies in 20–50-day filtered surface wind (m s^{-1}) and divergence (10^{-6} s^{-1}) before the onset of the Indian summer monsoon. Only anomalies that are significant at the 90% confidence level are shown.

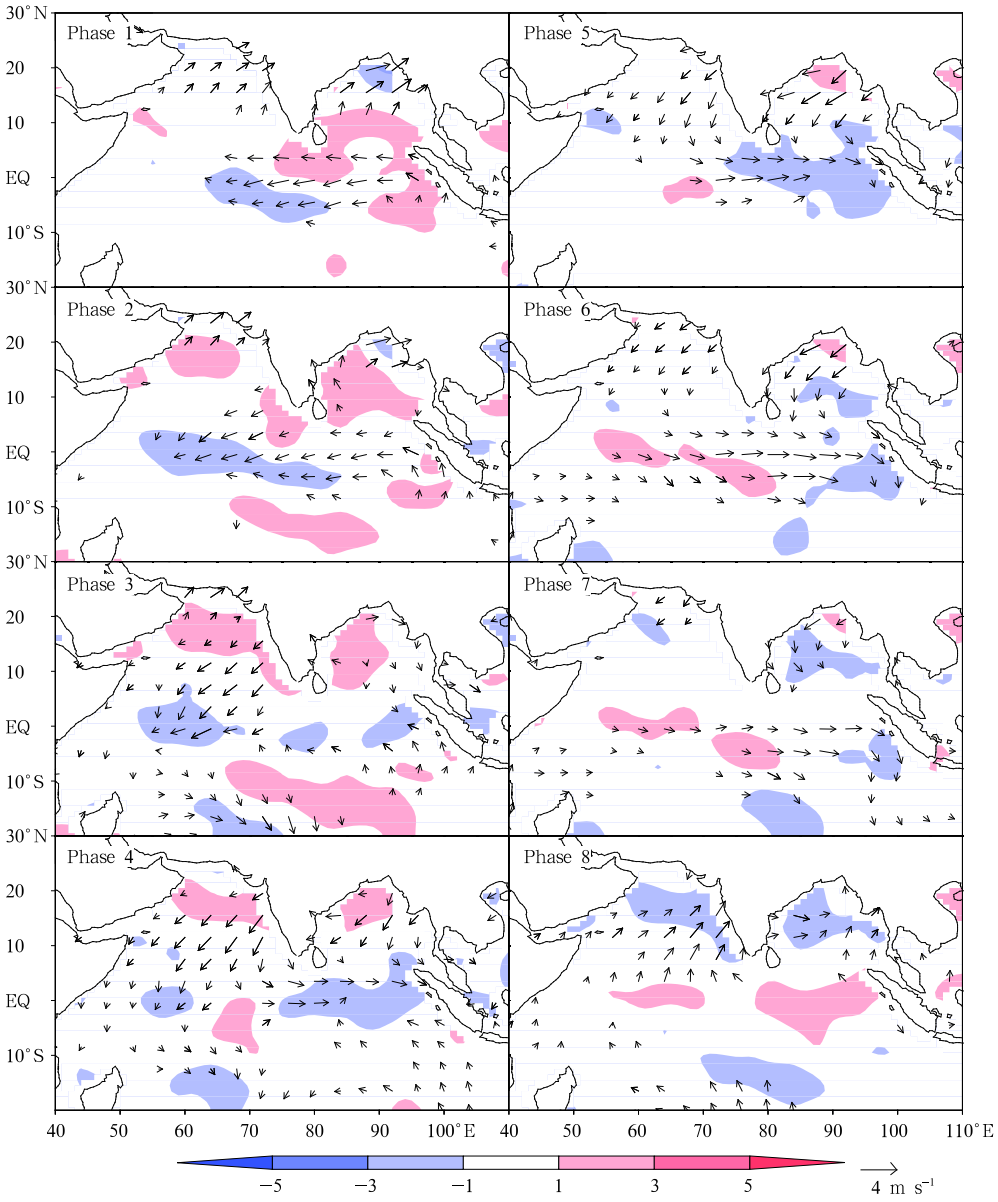

Fig. 6. As in Fig. 5, but for the situation after monsoon onset.

4.5 Vertical structure of ISO

4.5.1 Vertical structure of ISO along the equator

We use the same approach to compare and contrast the vertical structures of ISO before and after monsoon onset. Figures 7 and 8 show composite vertical distributions of vertical velocity and specific humidity along the equator (5°S–5°N) for each of the eight ISO phases. Anomalies in vertical motion and specific humidity propagate from west to east across the entire tropical Indian Ocean. The weakening of convection in Phase 1 corresponds to large-scale sinking motion over the equatorial Indian Ocean east of 70°E. The surface wind convergence in the western Indian Ocean during Phase 1 (Figs. 5 and 6) enhances water vapor concentration in the boundary layer to the west of 70°E. This moisture convergence promotes the development of convection in this region.

The phase-by-phase evolutions of vertical motion and specific humidity in ISO before and after monsoon

onset have several features in common. Positive anomalies in specific humidity during Phase 1 are located near the east coast of Africa, extending eastward to 60°–70°E. These specific humidity anomalies increase in magnitude and expand eastward along the equator in Phase 2, along with the appearance of upward motion in the lower troposphere (Fig. 7). This upward motion increases rapidly through Phase 3 and comes to dominate the entire equatorial Indian Ocean in Phase 4. The positive moisture anomalies continue to increase and expand eastward along the equator during this time, leading to an enhancement of convective precipitation. Convective activity in the eastern equatorial Indian Ocean peaks during Phase 5. The

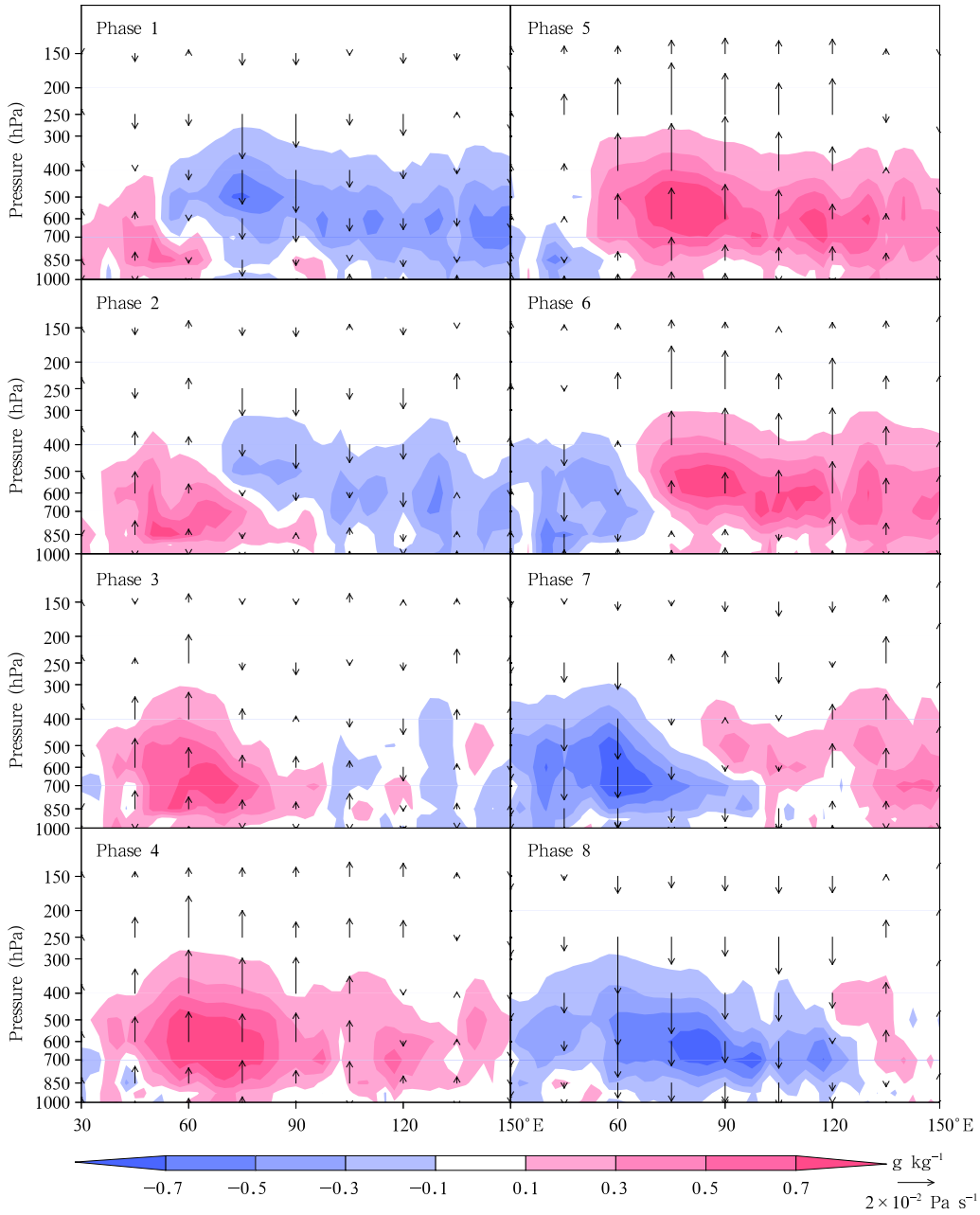

Fig. 7. Composite vertical structure of 20–50-day filtered vertical velocity (arrows; 10^{-2} Pa s^{-1}) and specific humidity anomalies (shading; g kg^{-1}) averaged between 5°S and 5°N for ISO before the onset of the Indian summer monsoon.

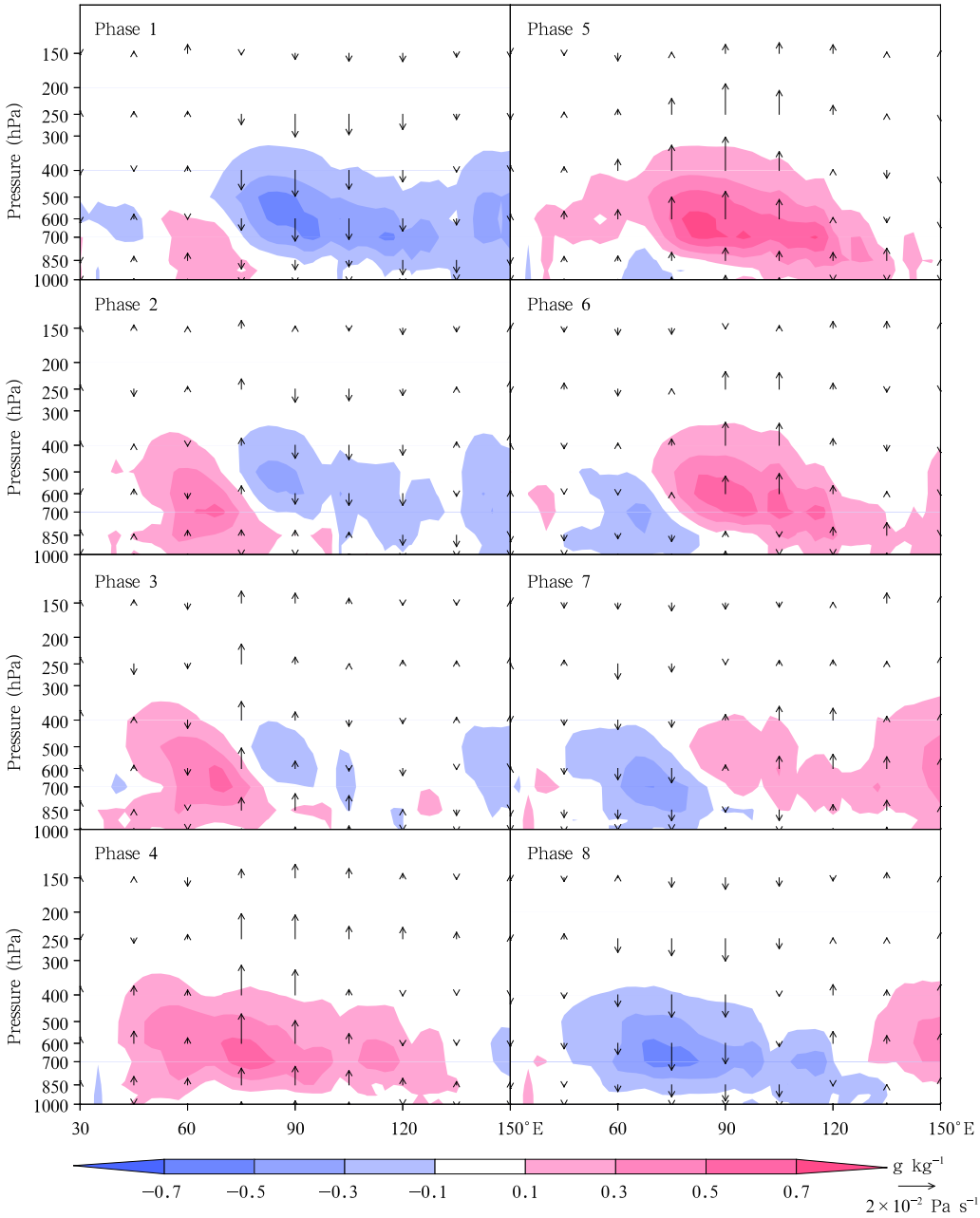

Fig. 8. As in Fig. 7, but for the situation after monsoon onset.

maximum upward motion is located at approximately 300 hPa, while the maximum specific humidity anomaly is located near 500 hPa. The decaying phases of ISO convection over the eastern Indian Ocean (Phases 6–8) feature reductions in upward motion along the equator associated with the northward movement of ISO precipitation. Sinking motion over the western Indian Ocean strengthens and moves eastward along the equator. Negative anomalies in specific humidity associated with near-surface divergence in the boundary layer over the eastern Indian Ocean also expand eastward during this time.

4.5.2 Vertical structure of ISO over the eastern Indian Ocean

Figures 9 and 10 show the composite vertical structures of anomalies in vertical motion and specific

humidity over the eastern Indian Ocean (zonal means averaged over 85°–95°E) before and after monsoon onset. ISO anomalies in both vertical motion and specific humidity propagate northward in this region during both periods. The troposphere over the eastern equatorial Indian Ocean is dry during Phase 1, with the largest negative specific humidity anomaly in the middle and lower troposphere. Vertical motion is predominantly downward to the south of 10°N. A positive anomaly in specific humidity begins to develop in the boundary layer, with the sinking motion shifting northward during Phases 1 and 2. Both upward motion and positive specific humidity anomalies increase significantly during the developing stages of ISO convection (Phases 3 and 4). These anomalies propagate both southward and northward from the equator, cor-

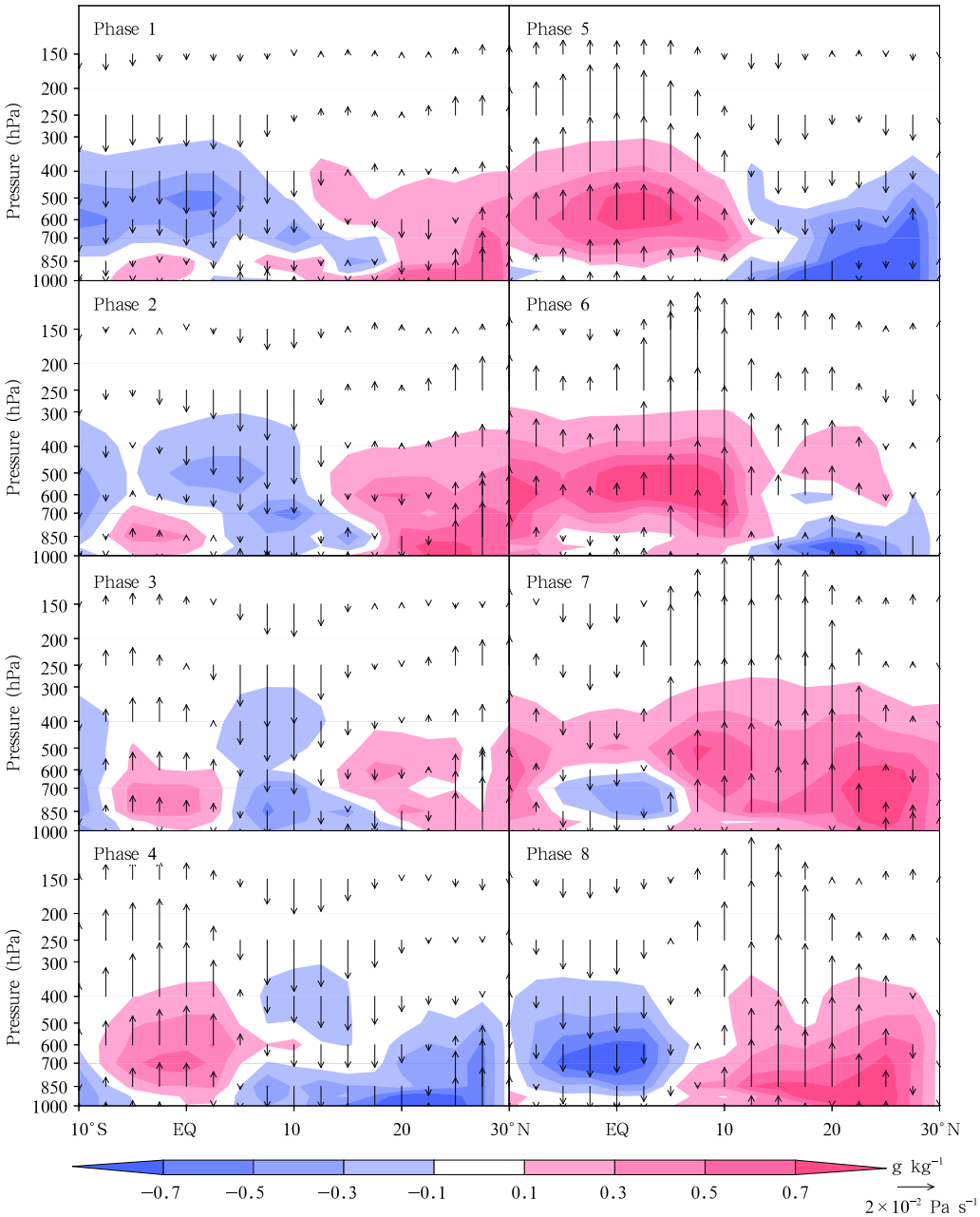

Fig. 9. Composite vertical structure of 20–50-day filtered vertical velocity (arrows; 10^{-2} Pa s^{-1}) and specific humidity anomalies (shading; g kg^{-1}) averaged between 85° and 95°E before the onset of the Indian summer monsoon.

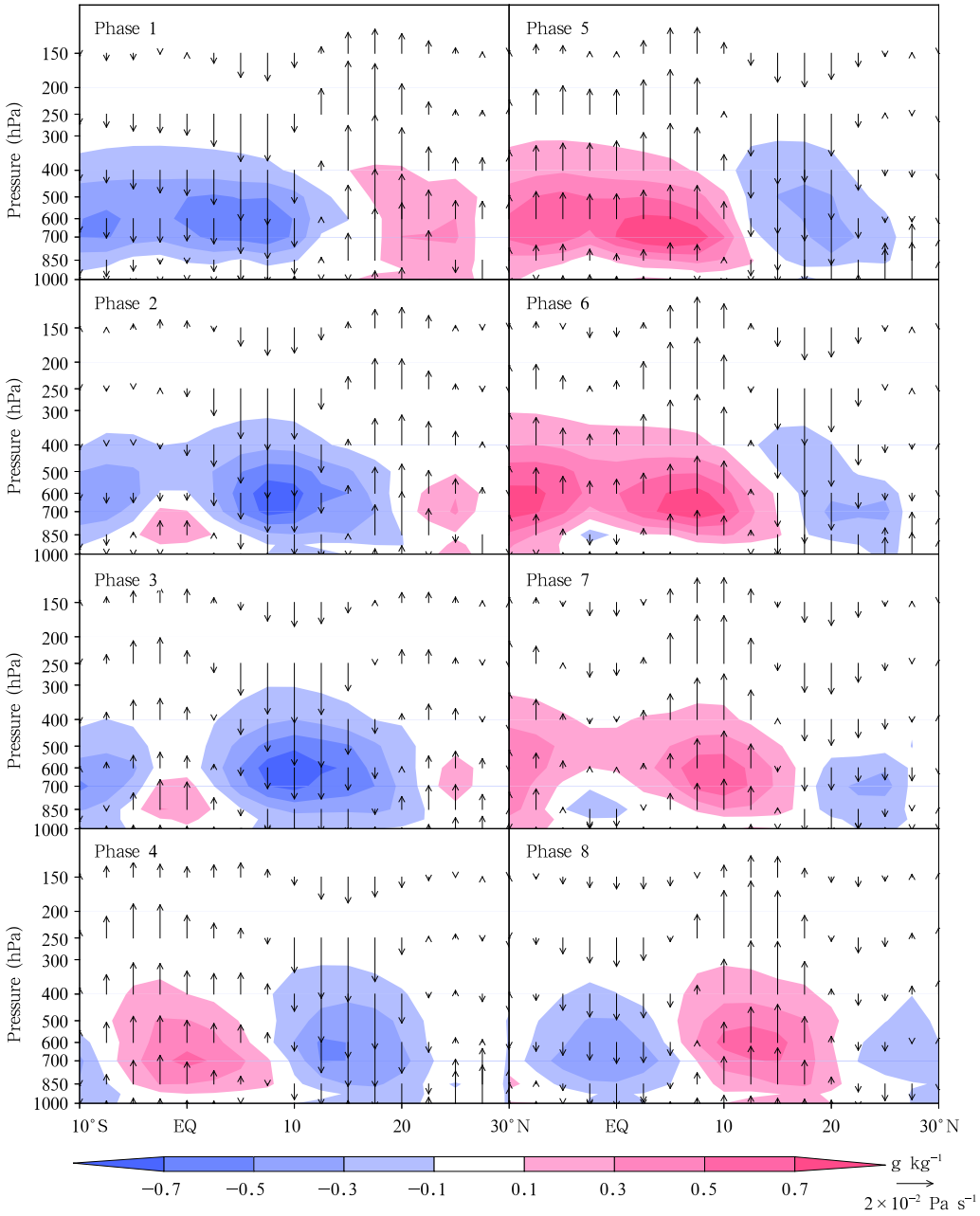

Fig. 10. As in Fig. 9, but for the situation after monsoon onset.

responding to the meridional movement of convection in the EEIO. Convective precipitation over the EEIO increases substantially during these stages as a result of surface wind convergence, which increases tropospheric moisture content and enhances upward motion. The moisture anomalies during the wet phase (Phase 5) are nearly opposite to those during Phase 1, with a deep layer of enhanced water vapor in the mid-lower troposphere below 300 hPa. The troposphere south of 10°N is characterized by strong upward motion during this stage of the ISO. Convection begins to weaken from Phase 6. Specific humidity and upward motion tend to decrease, with the positive anomalies shifting northward due to the propagation of the Rossby wave. Sinking motion and negative specific humidity anomalies appear near the equator during

Phase 7, re-establishing the dry phase (Phase 8) and setting the stage for the next ISO cycle.

The vertical structures of vertical motion and specific humidity anomalies evolve in similar ways before and after monsoon onset, but with some subtle differences. For instance, the positive specific humidity anomaly begins to develop in the boundary layer near 5°S during Phase 1 before onset of monsoon, but does not appear until Phase 2 after monsoon onset. Accordingly, the ISO convective precipitation anomaly over the EEIO occurs one phase later after monsoon onset (cf., Figs. 3 and 4).

5. Summary and discussion

In this study, we have compared the structure and evolution of ISO before and after the onset of the Indian summer monsoon using high-resolution satellite data and other observational data. The time series of 20–50-day filtered precipitation rate averaged over the eastern equatorial Indian Ocean is used as a reference to select strong ISO cases and construct composites of ISO behavior over the tropical Indian Ocean. We have focused on the general characteristics and vertical structure of the ISO during its life cycle, including the initiation, development, propagation, and decay of the ISO. We have presented and discussed differences in the evolution of ISO before and after monsoon onset. ISO convective precipitation anomalies appear first in the western equatorial Indian Ocean, and then intensify and expand eastward along the equator. Afterwards, these positive convective precipitation anomalies propagate northwestward and southwestward after reaching the EEIO. The northern branch is substantially stronger than the southern branch. The timing and location of the initial ISO convective precipitation anomalies after monsoon onset are different from those before monsoon onset. Before monsoon onset, positive precipitation anomalies associated with ISO initiate in the western equatorial Indian Ocean during Phase 2 and then propagate eastward along the equator. These precipitation anomalies initiate one phase later after monsoon onset, and their propagation has a much more pronounced northward component in the EEIO. Differences in the evolution of ISO convective precipitation anomalies before and after monsoon onset reflect differences in the background distributions of sea surface temperature and low-level specific humidity. Surface wind convergence and air-sea interactions play critical roles in initiating each new ISO cycle.

Differences in the structure and evolution of ISO in the tropical Indian Ocean between the periods before and after monsoon onset may be attributed to differences in ISO intensity and sea surface temperature anomalies. Anomalies in both ISO convective precipitation and sea surface temperature have greater amplitudes and larger areas before monsoon onset than after monsoon onset. The intensity of ISO over the tropical Indian Ocean has been shown to vary on subseasonal timescales (Kemball-Cook and Wang, 2001). Observations show that the variance and eastward propagation of ISO in the tropical Indian Ocean are both stronger during early summer (May–June) than during late summer (July–September). ISO anomalies in convective precipitation and associated SST anomalies are accordingly greater before the onset of the monsoon. By contrast, the convective activity and eastward propagation of ISO are weaker during late summer, after monsoon onset. The major ISO convective anomalies during late summer move northward into the Asian monsoon region, contributing to active and break cycles in monsoon rainfall.

Acknowledgments. The authors thank the anonymous reviewers for their valuable comments and suggestions. The language editor for this manuscript is Dr. Jonathon S. Wright.

REFERENCES

Fu, X. H., B. Wang, T. Li, et al., 2003: Coupling between northward propagating, intraseasonal oscillations, and sea-surface temperature in the Indian Ocean. *J. Atmos. Sci.*, **60**, 1733–1753.

Gadgil, S., 2003: The Indian monsoon and its variability. *Annu. Rev. Earth Planet. Sci.*, **31**, 429–467.

Goswami, B. N., and R. S. A. Mohan, 2001: Intraseasonal oscillations and interannual variability of the Indian summer monsoon. *J. Climate*, **14**, 1180–1198.

Guan Zhaoyong and Zhao Hui, 1995: Analysis of quasi-periodic disturbances of summer low-level flow field

with ECMWF long-term mean and 1980 data. *J. Nanjing Inst. Meteor.*, **18**(4), 518–522. (in Chinese)

Hartmann, D. L., M. L. Michelsen, and S. A. Klein, 1992: Seasonal variations of tropical intraseasonal oscillations: A 20–25-day oscillation in the western Pacific. *J. Atmos. Sci.*, **49**, 1277–1289.

Hendon, H. H., C. D. Zhang, and J. D. Glick, 1999: Interannual variation of the Madden-Julian oscillation during austral summer. *J. Climate*, **12**, 2538–2550.

Huang Ronghui, 1994: Interactions between the 30–60 day oscillation, the Walker circulation and the convective activities in the tropical western Pacific and their relations to the interannual oscillation. *Adv. Atmos. Sci.*, **11**(3), 367–384.

Jiang, X. N., T. Li, and B. Wang, 2004: Structures and mechanisms of the northward propagating boreal summer intraseasonal oscillation. *J. Climate*, **17**, 1022–1039.

——, and ——, 2005: Reinitiation of the boreal summer intraseasonal oscillation in the tropical Indian Ocean. *J. Climate*, **18**, 3777–3795.

Joseph, P. V., J. K. Eischeid, and R. J. Pyle, 1994: Interannual variability of the onset of the Indian summer monsoon and its association with atmospheric features, El Niño, and sea surface temperature anomalies. *J. Climate*, **7**, 81–105.

Ju Jianhua and Zhao Erxu, 2005: Impacts of the low frequency oscillation in East Asian summer monsoon on the drought and flooding in the middle and lower valley of the Yangtze River. *J. Trop. Meteor.*, **21**(2), 163–171. (in Chinese)

Kemball-Cook, S., and B. Wang, 2001: Equatorial waves and air-sea interaction in the boreal summer intraseasonal oscillation. *J. Climate*, **14**, 2923–2942.

Kripalani, R. H., A. Kulkarni, S. S. Sabade, et al., 2004: Intra-seasonal oscillations during monsoon 2002 and 2003. *Curr. Sci.*, **87**, 325–331.

Krishnamurti, T. N., and H. N. Bhalme, 1976: Oscillations of a monsoon system. Part I: Observational aspects. *J. Atmos. Sci.*, **33**, 1937–1954.

——, and D. Subrahmanyam, 1982: 30–50-day mode at 850 mb during MONEX. *J. Atmos. Sci.*, **39**, 2088–2095.

Lau, K. M., and P. H. Chan, 1986: Aspects of the 40–50-day oscillation during the northern summer as inferred from outgoing longwave radiation. *Mon. Wea. Rev.*, **114**, 1354–1367.

Lawrence, D. M., and P. J. Webster, 2001: Interannual variations of the intraseasonal oscillation in the South Asian summer monsoon region. *J. Climate*, **14**, 2910–2922.

Li, K. P., W. D. Yu, T. Li, et al., 2013: Structures and mechanisms of the first-branch northward-propagating intraseasonal oscillation over the tropical Indian Ocean. *Climate Dyn.*, **40**, 1707–1720.

Li, T., and B. Wang, 1994: The influence of sea surface temperature on the tropical intraseasonal oscillation: A numerical study. *Mon. Wea. Rev.*, **122**, 2349–2362.

——, ——, C. -P. Chang, et al., 2003: A theory for the Indian Ocean dipole-zonal mode. *J. Atmos. Sci.*, **60**, 2119–2135.

——, and ——, 2005: A review on the western North Pacific monsoon: Synoptic-to-interannual variabilities. *Terr. Atmos. Ocean Sci.*, **16**, 285–314.

Li Chongyin, Hu Ruijin, and Yang Hui, 2005: Intraseasonal oscillation in the tropical Indian Ocean. *Adv. Atmos. Sci.*, **22**, 617–624.

Lin, A. L., and T. Li, 2008: Energy spectrum characteristics of boreal summer intraseasonal oscillations: Climatology and variations during the ENSO developing and decaying phases. *J. Climate*, **21**, 6304–6320.

——, ——, Li Chunhui, et al., 2010: Relationships between interannual anomalies of sea surface temperature in the Indian Ocean and tropical boreal summer intraseasonal oscillations: Observations and simulations. *Acta Meteor. Sinica*, **68**(5), 617–630. (in Chinese)

——, ——, X. H. Fu., et al., 2011: Effects of air-sea coupling on the boreal summer intraseasonal oscillations over the tropical Indian Ocean. *Climate Dyn.*, **37**, 2303–2322.

Madden, R. A., and P. R. Julian, 1971: Description of a 40–50-day oscillation in the zonal wind in the tropical Pacific. *J. Atmos. Sci.*, **28**, 702–708.

——, and ——, 1972: Description of global-scale circulation cells in the tropics with a 40–50-day period. *J. Atmos. Sci.*, **29**, 1109–1123.

Mehta, A. V., and T. N. Krishnamurti, 1988: Interannual variability of the 30–50-day wave motions. *J. Meteor. Soc. Japan*, **66**, 535–548.

Murakami, T., 1976: Cloudiness fluctuations during the summer monsoon. *J. Meteor. Soc. Japan*, **54**, 175–181.

——, L. X. Chen, and A. Xie, 1986: Relationship among seasonal cycles, low-frequency oscillations, and transient disturbances as revealed from outgoing long-

wave radiation data. *Mon. Wea. Rev.*, **114**, 1456–1465.

Qi, Y. J., R. H. Zhang., T. Li, et al., 2008: Interactions between the summer mean monsoon and the intraseasonal oscillation in the Indian monsoon region. *Geophys. Res. Lett.*, **35**, L17704, doi: 10.1029/2008GL034517.

——, ——, ——, et al., 2009: Impacts of intraseasonal oscillation on the onset and interannual variation of the Indian summer monsoon. *Chinese Sci. Bull.*, **54**, 880–884.

Rao, S. A., and T. Yamagata, 2004: Abrupt termination of Indian Ocean dipole events in response to intraseasonal disturbances. *Geophys. Res. Lett.*, **31**, L19306. doi: 10.1029/2004GL020842.

Shukla, J., and D. A. Paolino, 1983: The southern oscillation and long-range forecasting of the summer monsoon rainfall over India. *Mon. Wea. Rev.*, **111**, 1830–1837.

Sikka, D. R., and S. Gadgil, 1980: On the maximum cloud zone and the ITCZ over Indian, longitudes during the Southwest monsoon. *Mon. Wea. Rev.*, **108**, 1840–1853.

Teng, H. Y., and B. Wang, 2003: Interannual variations of the boreal summer intraseasonal oscillation in the Asian–Pacific region. *J. Climate*, **16**, 3572–3584.

Wang, B., and H. Rui, 1990: Synoptic climatology of transient tropical intraseasonal convection anomalies: 1975–1985. *Meteor. Atmos. Phys.*, **44**, 43–61.

——, and X. S. Xie, 1996: Low-frequency equatorial waves in vertically sheared zonal flow. Part I: Stable waves. *J. Atmos. Sci.*, **53**, 449–467.

——, and ——, 1997: A model for the boreal summer intraseasonal oscillation. *J. Atmos. Sci.*, **54**, 72–86.

——, and X. H. Xu, 1997: Northern Hemisphere summer monsoon singularities and climatological intraseasonal oscillation. *J. Climate*, **10**, 1071–1085.

——, P. J. Webster, and H. Y. Teng, 2005: Antecedents and self-induction of active-break south Asian monsoon unraveled by satellites. *Geophys. Res. Lett.*, **32**, L04704, doi: 10.1029/2004GL020996.

——, P. J. Webster, K. Kikuchi, et al., 2006: Boreal summer quasi-monthly oscillation in the global tropics. *Climate Dyn.*, **27**, 661–675.

Webster, P. J., A. M. Moore, J. P. Loschnig, et al., 1999: Coupled ocean-atmosphere dynamics in the Indian Ocean during 1997–1998. *Nature*, **401**, 356–360.

Yang Yanjuan, Guan Zhaoyong, and Zhu Baolin, 2007: Possible influences of the Indian Ocean dipole on the intensity of intraseasonal oscillation in Boreal summer. *J. Nanjing Inst. Meteor.*, **30**(2), 224–230. (in Chinese)

Yasunari, T., 1979: Cloudiness fluctuations associated with the Northern Hemisphere summer monsoon. *J. Meteor. Soc. Japan*, **57**, 227–242.

——, 1980: A quasi-stationary appearance of 30–40 day period in the cloudiness fluctuations during the summer monsoon over India. *J. Meteor. Soc. Japan*, **58**, 225–229.

Zhan, R., J. Li, and A. Gettelman, 2006: Intraseasonal variations of upper tropospheric water vapor in Asian monsoon region. *Atmos. Chem. Phys. Discuss*, **6**, 8069–8095.

Zhu, C. W., T. Nakazawa, J. P. Li, et al., 2003: The 30–60 day intraseasonal oscillation over the western North Pacific Ocean and its impacts on summer flooding in China during 1998. *Geophys. Res. Lett.*, 30, doi: 10.1029/2003GL017817.